JOURNAL OF SOLID STATE CHEMISTRY 55, 251–261 (1984)

Structural Intergrowth in the $Ca_xLa_{1-x}FeO_{3-x/2}$ System ($0 \leq x \leq 1$): An Electron Microscopy Study

MARÍA VALLET-REGÍ, JOSÉ GONZÁLEZ-CALBET, AND MIGUEL A. ALARIO-FRANCO*

Departamento de Química Inorgánica and Instituto "Elhuyar," CSIC, Facultad de Ciencias Químicas, Universidad Complutense, Madrid-3, Spain

AND JEAN-CLAUDE GRENIER AND PAUL HAGENMULLER

Laboratoire de Chimie du Solide du CNRS, 351, cours de la Libération, 33405 Talence Cedex, France

Received December 19, 1983; in revised form May 22, 1984

An electron microscopy and diffraction study of several samples of the system $Ca_xLa_{1-x}FeO_{3-x/2}$ shows these solids to be formed by the disordered intergrowth of two out of three of the ordered terms corresponding to $x = 0$, $x = \frac{2}{3}$, and $x = 1$ (i.e., $LaFeO_3$, $Ca_2LaFe_3O_8$, and $Ca_2Fe_2O_5$). The relative amounts of the intergrowing individuals vary with x and may extend down to unit cell thickness; i.e., to the level of isolated extended defects.

Introduction

Among the various ways that solids use to accommodate compositional variations (*1*), the intergrowth of simple structures (*2*) is relatively frequent. That is indeed the case for some anion-deficient perovskites (*3*) where the close analogy (*4*) that exists between $A_2M_2O_5$ brownmillerite (*5*) and AMO_3 perovskite (*6*) structures allows an intermediate composition $AMO_{8/3}$ to exist (*7, 8*) with a structure which derives indeed from the limiting structures (*9, 10*).

As it is well known (*11, 12*) the brownmillerite structure can be described with an ordered sequence of alternating octahedral and tetrahedral "layers," while in the perovskite structure only octahedra are present. The $AMO_{2.67}$ family of phases (*13*) is believed to have a structure formed by an alternating sequence of two octahedral and one tetrahedral layers (*9, 10*). Such a sequence can in fact be considered as an ordered intergrowth between a perovskite cell and half a brownmillerite unit cell.

Other sequences are indeed possible and the compound $Ca_4YFe_5O_{13}$, corresponding to a composition $AMO_{2.60}$, has been shown (*14*) to present a related, although more complex sequence of octahedral and tetrahedral layers including twinning at the unit cell level.

Although these phases can all be considered as members of a common structural

* To whom correspondence should be addressed.

0022-4596/84 $3.00

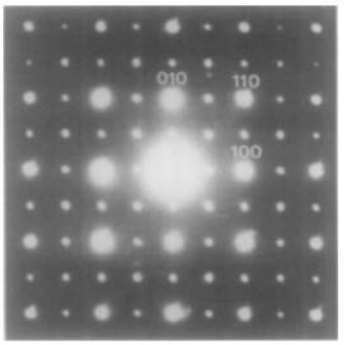

FIG. 1. Electron diffraction pattern of the $x = 0.2$ sample along $[001]_c$ showing the apparent doubling of the perovskite cell in both a^* and b^* directions.

series of general formulation $A_nM_nO_{3n-1}$, in which they are the members corresponding to $n = 2, \frac{5}{2}, 3$, and ∞, no other member seems to occur. In order to clarify the situation, we have performed a study by electron microscopy and diffraction of a number of samples having various compositions within the system "$Ca_xLa_{1-x}FeO_{3-x/2}$."[1]

We describe and discuss below the results of this study.

Experimental

Samples were prepared from a stoichiometric mixture of La_2O_3, $CaCO_3$, and $Fe(NO_3)_3 \cdot 9H_2O$ dissolved in dilute nitric acid. The corresponding nitrates were decomposed at low temperature and refired in air for 3 days at 1350°C. All samples were then annealed at 1100°C under low oxygen pressure ($pO_2 < 10^{-6}$ atm). Chemical analyses indicated that iron was exclusively in a +III oxidation state. Powder X-ray characterization was performed on a Guinier–Hägg-type camera. Full details of these procedures have been given earlier (*7, 8, 15*).

Electron microscopy and diffraction were performed on a Siemens Elmiskop 102. The samples were ultrasonically dispersed in *n*-butanol and then transferred to carbon-coated copper grids.

[1] For this notation see final discussion and Fig. 8.

Results

According to a previous X-ray study, the $x = 0.2$ sample was orthorhombic and has a cell volume slightly smaller than that of $LaFeO_3$ ($x = \phi(LaFeO)_3$: $V = 243.02$ Å^3 (*16*); $x = 0.2$: $V = 237.08$ Å^3).

By electron diffraction both samples gave patterns that at first sight, could be indexed in a doubled perovskite cell. Figure 1 shows an example along the $[001]_c$ axis.[2] However, electron microscopy showed that the situation corresponded actually to multitwinned crystals. In each of the individuals the doubled perovskite axis characteristic of the $a_c\sqrt{2} \cdot a_c\sqrt{2} \cdot 2a_c$ $LaFeO_3$-like cell (*16*) was at random in one of the three space directions. Figure 2a shows a micrograph of an area of a crystal in which three individuals coexist. Regions marked X, Y, and Z correspond to the individuals giving the diffraction patterns shown in Figs. 2b, c, and d, respectively. It is clear that a selected area diaphragm covering the region of contact of the three types of domains will give patterns similar to that shown in Fig. 1. It is worth pointing out that the slight distortion ($a = 5.553(2)$, $b = 5.563(2)$, $c = 7.867(3)$) (*16*) is not obvious in powder X-ray diffraction patterns (*16–20*) or in electron diffraction patterns. Thus, it is really because this orthorhombic distortion is so small, that three-dimensional twinning is observed.

A final point worth of note in those samples is the lack of regularity of the compositional boundaries C_{XY}, C_{XZ}, and C_{YZ} in Fig. 2a. The kind of multitwinning observed in the $x = 0$ and $x = 0.2$ compositions is similar to that optically observed for $YAlO_3$ (*17*), but at a much finer scale.

[2] Subindex c refers to the cubic perovskite unit cell. Subindexes o and G refer to the $LaFeO_3$ and $Ca_2LaFe_3O_3$-type unit cells, respectively.

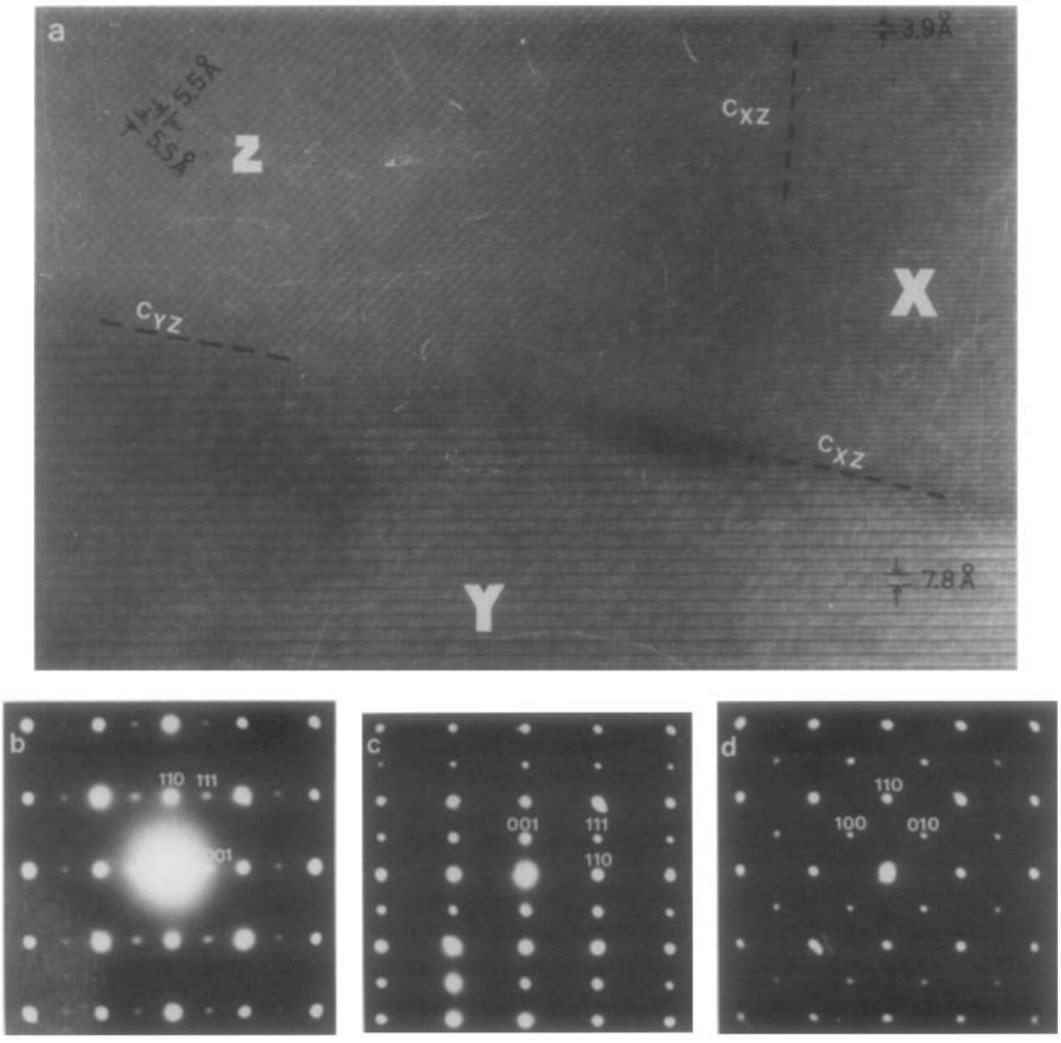

FIG. 2. (a) Electron micrograph showing multitwinning in the $x = 0$ sample ($LaFeO_3$). (b, c, and d) Electron diffraction patterns corresponding to individuals X, Y, and Z, respectively. Indexes refer to the $LaFeO_3$-type unit cell.

Introducing more calcium in $LaFeO_3$, considerably diminishes the intensity of the X-ray superstructure lines and only relatively broad peaks corresponding to a simple cubic subcell were observed in the X-ray diffraction pattern of the $x = 0.4$ sample, i.e., "$Ca_{0.40}La_{0.60}FeO_{2.80}$," whose unit cell parameter was $a_c = 3.882(2)$ Å. By electron microscopy and diffraction the real situation appeared much more complex and two types of solids were observed to exist. They were both formed by a disordered intergrowth and, although the intergrowing individuals were in both cases the same, their relative amounts were different.

Figure 3a shows an electron diffraction pattern characteristic of one of the two types of intergrowth; three kinds of diffraction maxima can be recognized: (a) a set of strong reflexions, corresponding to a simple

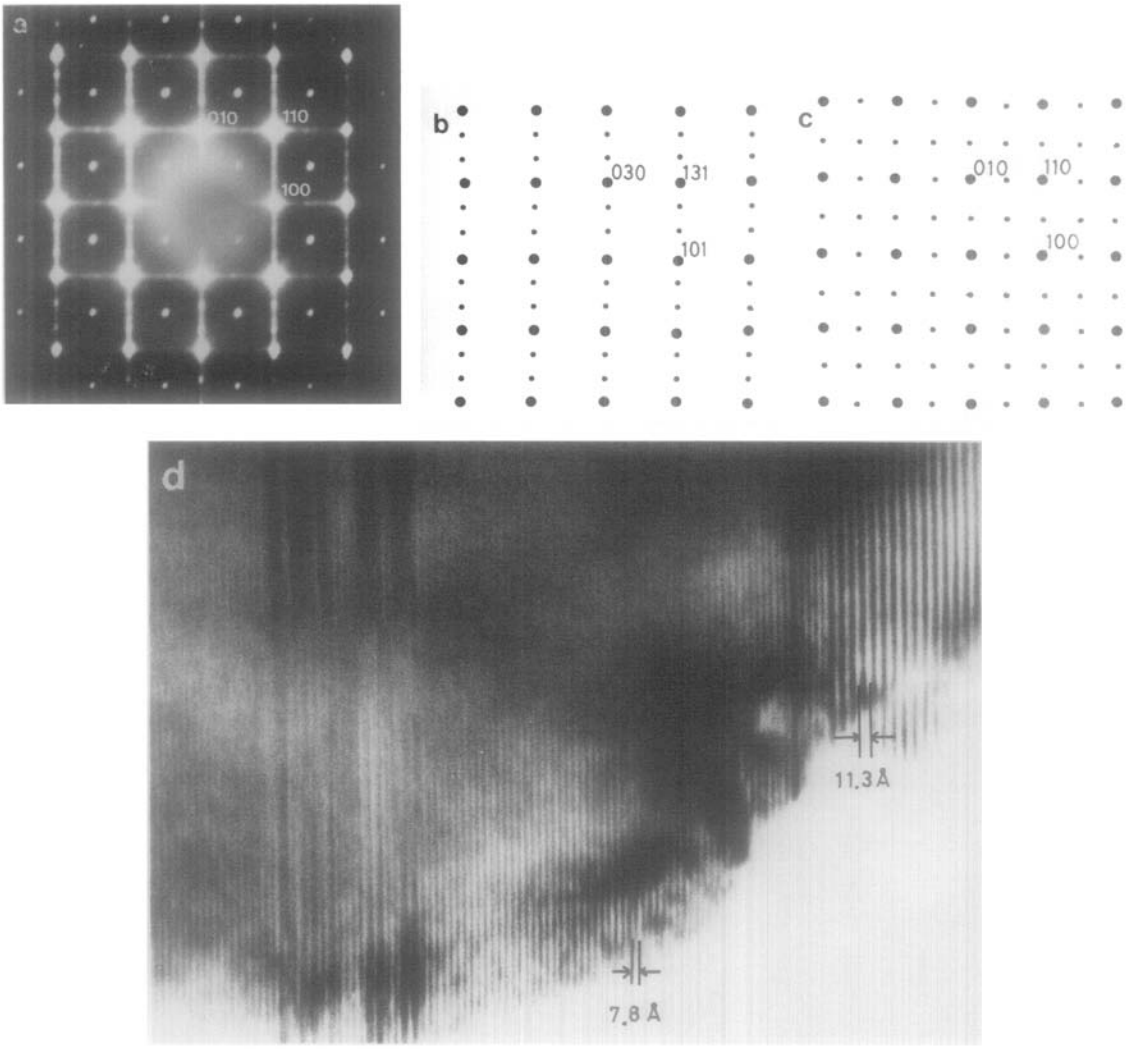

FIG. 3. (a) Electron diffraction pattern of one of the $x = 0.4$ samples (see text). It is characterized by the superposition of two patterns which can be indexed as $[101]_G$ as in (b) and $[001]_o$ as in (c). Marked streaking is apparent. (d) Corresponding electron micrograph showing the intergrowth of regions characterized by a $d_{010_G} \simeq 11.3$ Å spacing with other regions characterized by the $d_{001_o} \simeq 7.8$ Å spacing of the $LaFeO_3$-type cell.

cubic perovskite substructure along the $[001]_c$ axis (unit cell $\simeq a_c \times a_c \times a_c$); (b) another set of maxima which can be indexed in the $[10\bar{1}]_G$ zone axis of the $Ca_2LaFe_3O_8$ unit cell ($a_G \simeq a_c\sqrt{2}$; $b_G \simeq 3a_c$; $c_G \simeq a_c\sqrt{2}$) schematically shown in Fig. 3b. In the following, this cell will be referred to by subindex G; (c) a third group of maxima which can be indexed as in Fig. 1 above, schematically shown in Fig. 3c.

The corresponding electron micrograph, in Fig. 3d, shows that these crystals are formed by a disordered intergrowth between regions characterized by the $\simeq 11.3$ Å $= d_{010_G}$ spacing of $Ca_2LaFe_3O_8$ and other regions where the fringe periodicity corre-

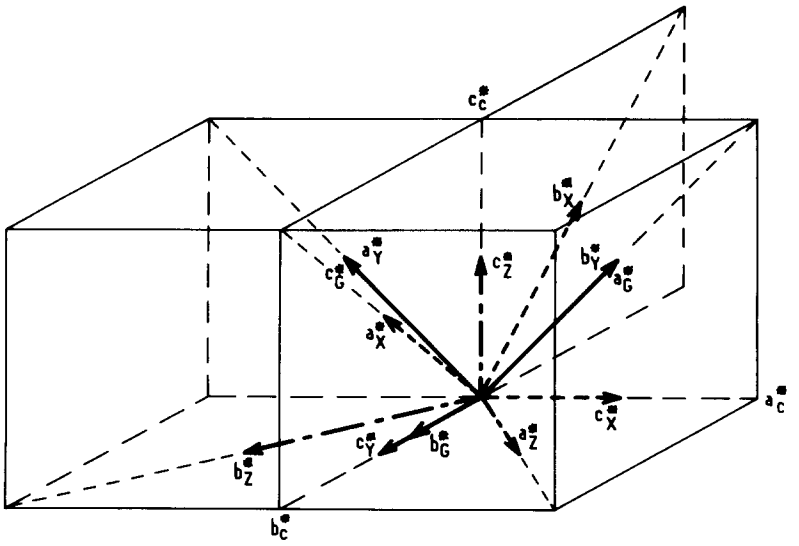

FIG. 4. Relative orientation of the axes of the four reciprocal cells corresponding to the $x = 0.4$ sample.

sponds to the $d_{010_o} \simeq 7.8$ Å spacing of the $LaFeO_3$-type cell. A closer observation of Figs. 3a, b, and c reveals that the strong subcell reflexions appear at the reciprocal positions where the diffraction maxima of sets (b) and (c) coincide. This is certainly due to the fact that those two structures are superstructures of the basic perovskite cell. The ensemble of these observations suggests then that the relative orientation of the axes of the four reciprocal cells of the crystal can be schematized as in Fig. 4.

The other type of samples having the same nominal composition, $x = 0.4$, showed diffraction patterns that were *geometrically analogous* to those just described. However, the relative intensities differed markedly from the above patterns. Figure 5a gives a typical example. It can be seen that besides the predominant substructure spots, the diffraction maxima belonging to the $Ca_2LaFe_3O_8$ reciprocal cell are far less intense than those corresponding to the doubled pervoskite reciprocal cell. The electron micrograph relative to such a sample in this orientation (Fig. 5b), explains the origin of the intensity differences. It can be observed that, dispersed within a set of fringes of spacing $\simeq$3.9 Å there appear isolated fringes with a width of $\simeq$11.3 Å. These thicker fringes correspond to isolated lamellae of the $Ca_2LaFe_3O_8$ structure aperiodically dispersed within the doubled perovskite structure in which they are coherently intergrown. They are examples of Wadsley defects (*21*) (see the discussion below). It is worthwhile to mention that, although most of these defects start at the crystal edge and end within the crystal, some of them, like those indicated by arrows in Fig. 5b, start and end within the crystal.

It is also worth pointing out that the true periodicity along the c_o axis of the $LaFeO_3$ type matrix (7.8 Å), is only imaged in the thicker regions of the crystals (*22*). Some of these regions have been indicated in Fig. 5b.

Yet another group of crystals of the same analytical composition showed the intergrowth along $[110]_o//b_G$, so that the corresponding micrographs showed the $LaFeO_3$-

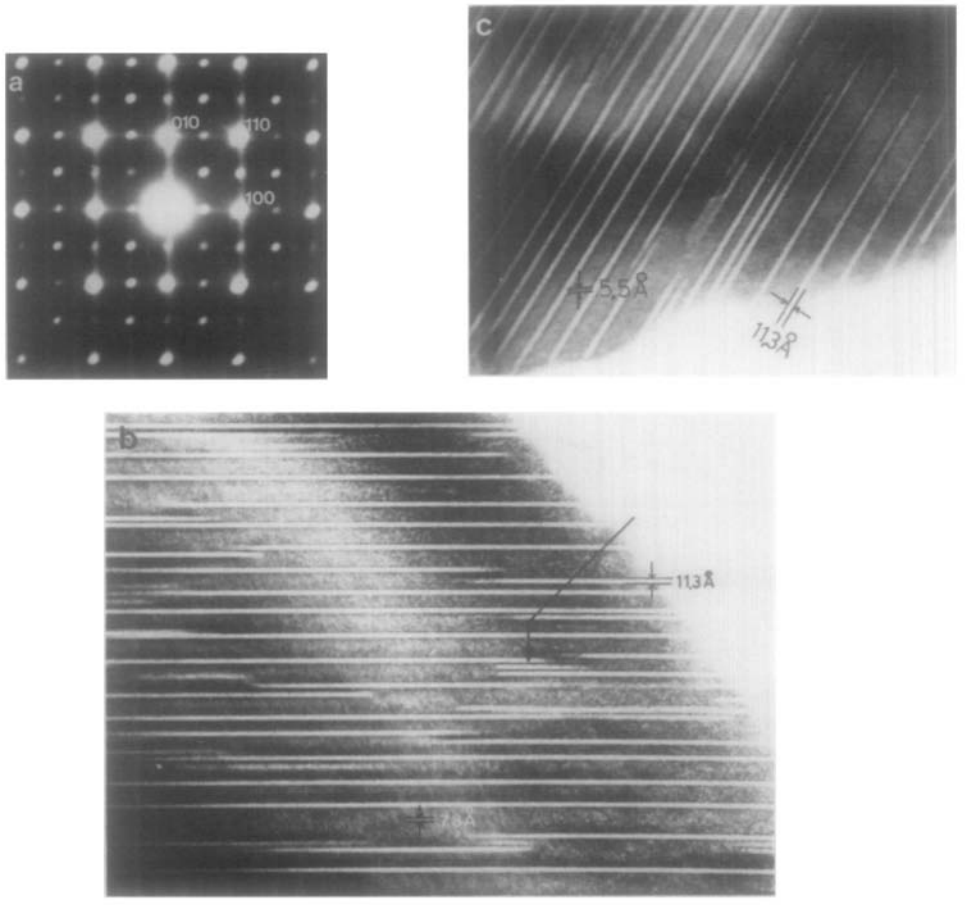

FIG. 5. (a) Electron diffraction pattern of another $x = 0.4$ sample (see text) along the $[001]_c$ zone axis. (b) Corresponding micrograph. The presence of isolated extended defects is apparent (compare with Fig. 3d). (c) Electron micrograph corresponding to a third type of $x = 0.4$ crystals where the intergrowth is along $[110]_{o//b_G}$.

type domains along $[001]_o$. An example is given in Fig. 5c.

X-Ray diffraction work on the $x = 0.5$ and $x = 0.6$ samples provided complex patterns that were difficult to index in terms of either $LaFeO_3$ (o)—or $Ca_2LaFe_3O_8$ (G) cells.

The electron diffraction patterns corresponding to $x = 0.6$, were again geometrically similar but the more intense spots, besides those of the substructure, corresponded to the $Ca_2LaFe_3O_8$ structure. Figure 6a shows a typical electron diffraction pattern which can be indexed as $(001)_c//(10\bar{1})_G$. Marked streaking of the diffraction spots, suggesting the existence of disorder can be observed in this diagram along both b_G^* and c_o^*. Figure 6b shows the corresponding electron micrograph. Again, two types of fringes are seen, with fringe spacings mostly equal to 11.3 Å = d_{010_G}, but sometimes of ≃3.9 Å = d_{002_o}. An interesting point regarding this $x = 0.6$ sample is that the fringe periodicity extends in relatively large areas for each of the individual components.

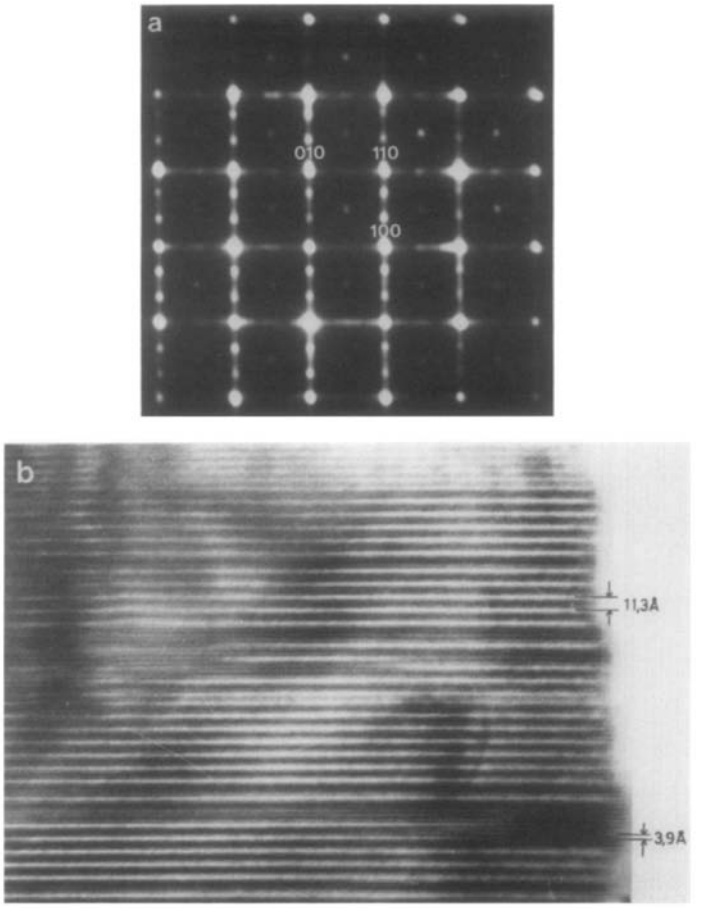

FIG. 6. (a) Electron diffraction pattern of the $x = 0.6$ sample indexed along the $[001]_c$ zone axis. (b) Corresponding micrograph: an intergrowth is obvious.

When $x = 0.67$, no disordered intergrowth is present. As Figs. 7a and b show clearly by electron diffraction and electron microscopy, only one phase is present: $Ca_{0.67}La_{0.33}FeO_{2.67}$, i.e., $Ca_2LaFe_3O_8$. Neither streaking in the diffraction pattern nor faults in the periodicity are visible. There are, however, noticeable differences in constrast all over the picture; they certainly result from differences in crystal thickness and the consequent variations in focusing conditions over the different crystal regions (*23*). As expected from the diffraction pattern, fringe periodicities correspond to $\simeq$11.30 Å $\times$ 3.9 Å. In order to keep a consistent orientation in all the images given in this paper, Figs. 7a and b, corresponding to $Ca_2LaFe_3O_8$, are in the $[10\bar{1}]_G$ zone axis. However, this projection is less illustrative of the sequence of octahedral and tetrahedral layers characteristic of the $Ca_2LaFe_3O_8$ structure than the more usual $[100]_G$ projection, parallel to the $[10\bar{1}]_c$ axis of the subcell (*10*).

For the samples corresponding to $\frac{2}{3} < x < 1$, a previous detailed study has given evidence of disordered intergrowth between $Ca_2Fe_2O_5$ (brownmillerite) and $Ca_2LaFe_3O_8$ (G phase) (see Fig. 2 of Ref. (*10*)). The relative amounts of the end members change

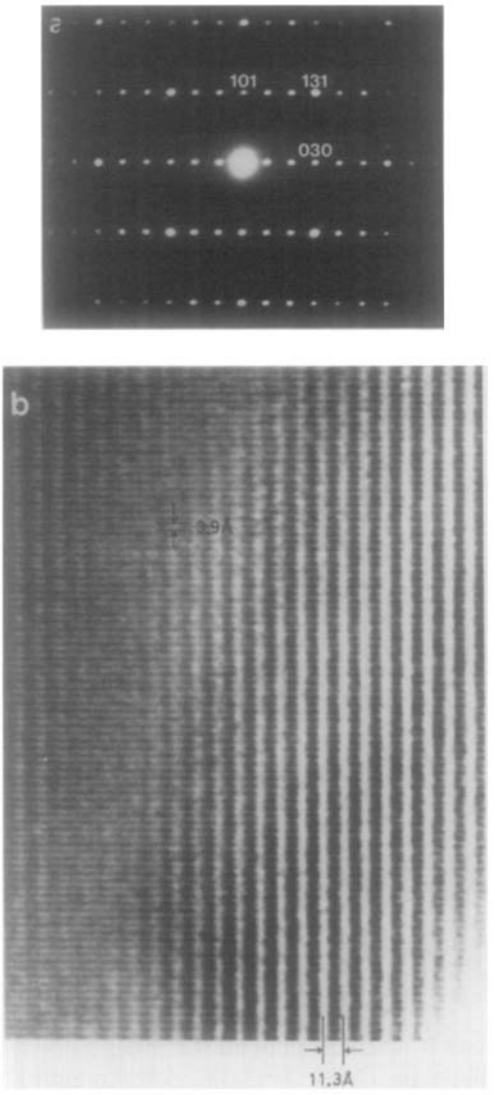

FIG. 7. (a) Electron diffraction pattern of the $x = \frac{2}{3} \simeq 0.67$ sample. (b) Corresponding micrograph.

according to the nominal composition. Moreover, it was given evidence of two types of intergrowth boundaries.

A previous study of the Mössbauer spectra of these samples (15) indicated that, except for low calcium concentration, i.e., $x < 0.1$, there appear two Zeeman splittings with chemical shifts of $\simeq$0.37 and $\simeq$0.19 mm/sec, respectively, with hyperfine fields of the order of 510 and 420 kOe. These values are analogous to those observed for $Ca_2Fe_2O_5$ (*24*) and $Ca_2LaFe_3O_8$ (*8*) and can be attributed to Fe(3+) ions in octahedral and tetrahedral sites. For $x \simeq 0.1$ however only a sextuplet could be observed; this is also the case for $LaFeO_3$ (*25*). According to the relative intensities in the spectra, the ($Fe^{III}O_4$) sextuplet vanishes as x decreases, indicating a diminishing number of tetrahedrally surrounded Fe(3+) ions with increasing lanthanum content.

Discussion

The above results show that, although $Ca_2LaFe_3O_8$ can be considered as an ordered intermediate phase existing between perovskite and brownmillerite a possibility of forming other ordered sequences of octahedral and tetrahedral layers in the $A_nM_nO_{3n-1}$ series is difficult to meet in practice. In this way, the annealed samples corresponding to compositions other than $x = 0$, $\frac{2}{3}$ or 1, within the so-called solid solution "$Ca_xLa_{1-x}FeO_{3-x/2}$" are actually constituted by an intergrowth of two out of three of the oxides: $LaFeO_3$, $Ca_2LaFe_3O_8$, and $Ca_2Fe_2O_5$, whose chemical formula can be expressed, in terms of perovskite compositions, as AMO_3, $AMO_{2.67}$, and $AMO_{2.5}$, respectively.

Why this is so, or in other words, why $Ca_2LaFe_3O_8$ is apparently the only stable intermediate term in these series at least in annealed samples, is not clear. It is probable that computer simulation techniques like those developed by Catlow *et al.* (*26*) or Parker (*27*) will help to understand this point. However, independently from the reasons of such a behavior, their implications are that compositional variations in the samples of a system containing only trivalent iron are governed by the Ca/La ratio and reflected in the relative amounts of the corresponding end members intergrown in

a disordered way within each crystal. The electron micrographs reflect nicely the nominal compositions. Although there was no attempt to make a quantitative estimation, it is clear that the $x = 0.6$ sample should be richer for instance in the $Ca_2LaFe_3O_8$ component, as its nominal or analytical composition "$Ca_{0.60}La_{0.40}FeO_{2.70}$" is equivalent to ($LaFeO_3 + 3Ca_2LaFe_3O_8$); Fig. 6b approximately shows such relative amounts. On the contrary, the $x = 0.2$ sample should contain a larger proportion of the $LaFeO_3$ component, since it has a nominal composition "$Ca_{0.20}La_{0.80}FeO_{2.90}$" equivalent to ($7LaFeO_3 + Ca_2LaFe_3O_8$); for this reason, pictures such as Fig. 2 corresponding to this sample will essentially show $LaFeO_3$-type images. It is however to be noticed that we have not observed any $Ca_2LaFe_3O_8$-type region in the $x = 0.2$ crystals. This formal composition implies about 3% of oxygen vacancies and it has been previously shown (*13*) that the oxygen vacancies are arranged into finite files which are randomly dispersed within the network. It is then not surprising that $Ca_2LaFe_3O_8$ regions do not appear in the microscope images for this composition.

For intermediate samples such as $x = 0.4$ whose composition "$Ca_{0.40}La_{0.60}FeO_{2.80}$" is equivalent to ($2LaFeO_3 + Ca_2LaFe_3O_8$) an intermediate, albeit heterogeneous, situation occurs in fact. We have found in this sample two types of crystals: some of them, as exemplified in Fig. 5b, show an intergrowth of Wadsley defects within a $LaFeO_3$-type matrix; others, however, present a more balanced intergrowth between both limiting phases. As both types of crystals were detected in the same batch one is tempted to attribute its existence to kinetic reasons.

When the composition of the "solid solution" approaches $x = \frac{2}{3}$ the $Ca_2LaFe_3O_8$ phase increases and this is indeed the only phase observed for this value. However, we did not observe in any case isolated lamellae of $LaFeO_3$ within a $Ca_2LaFe_3O_8$ matrix.

In the $\frac{2}{3} < x < 1$ range we have previously shown the existence of a disordered intergrowth between $Ca_2Fe_2O_5$ and $Ca_2LaFe_3O_8$ phases.

The Mössbauer spectra corresponding to all these samples have been fully discussed elsewhere by Grenier *et al.* (*8, 15*). They illustrate clearly the evolution of the system in terms of local environment of the iron ions as far as both oxidation state and coordination number are concerned. However, they do not provide information about the way in which these local environments are distributed all over the crystal. In this context, it is obvious that the use of electron diffraction and even more of electron microscopy may be recommended for studying this type of systems.

In the light of the above observations and others previously made (*1, 2, 10*) it is clear that phase mixtures of materials that are structurally related and have close compositions will seldom appear. Under such circumstances a structural intergrowth is obviously a more appropriate situation.

The phenomenon of intergrowth is indeed not new and under different denominations has more or less explicitly been used to explain either compositional variations or the presence of defects or even both together. In this way Sato (*28*) called *Syntatic Intergrowth* the "intergrowth in narrow bands" and reserved the term *Microsyntaxy or Microsyntactic Intergrowth* to the case where intergrowth came "down to the unit cell scale" (*29, 30*). In the last eventuality other terms like *sequence fault* (*31*) or *sequential faults* (*32*) have also been used. We suggest that the term *Wadsley defect,* although corresponding specifically to an isolated lamella of unit cell thickness of a crystallographic shear phase intergrown within a crystal matrix (*21, 23*) should be extended to the more general case of any structural intergrowth of unit cell thick-

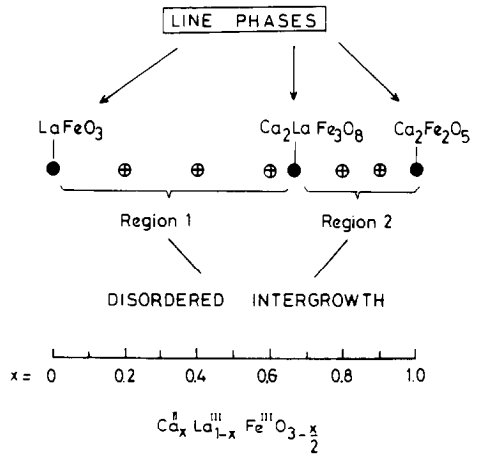

FIG. 8. Tentative phase diagram for the $Ca_x La_{1-x}Fe^{III}O_{3-x/2}$ system at 1100°C as deduced from the electron microscopy investigations.

ness. In this way, the isolated extended defects observed in Fig. 5b should be considered as Wadsley defects (WD).

In the present "$Ca_xLa_{1-x}FeO_{3-x/2}$" system under reducing conditions instead of having "compounds" (*34*), *"phase mixtures"* (*35*), or *"simple solid solution"* we have observed disordered intergrowths between the *"line phases"*: $Ca_2Fe_2O_5$, $Ca_2LaFe_3O_8$, and $LaFeO_3$. Figure 8 schematically shows a tentative phase diagram at 1100°C for these ferrites (III).

This certainly does not mean that such oxides are incapable to show nonstoichiometry. This actually happens under appropriate conditions for at least the first two of them in a quite sophisticated way by means of microdomain formation (*36, 37*).

Acknowledgments

We thank Dr. M. Marezio for valuable comments and L. Puebla, A. García, and A. Wattiaux for technical assistance.

References

1. L. EYRING, *in* "Nonstoichiometric Oxides" (O. T. Sorensen, Ed.), Chap. 7, p. 337, Academic Press, New York (1981).
2. S. IIJIMA AND J. ALLPRESS, *Acta Crystallogr. Sect. A* **30,** 29 (1974).
3. J. C. GRENIER, J. DARRIET, M. POUCHARD, AND P. HAGENMULLER, *Mater. Res. Bull.* **11,** 1219 (1976).
4. D. A. WADSLEY, *in* "Nonstoichiometric Compounds" (L. Mandelcorn, Ed.), Chap. 3, p. 135, Academic Press, New York (1964).
5. E. F. BERTAUT, P. BLUM, AND A. SAGNIERES, *Acta Crystallogr.* **12,** 149 (1959).
6. H. D. MEGAW, *Proc. Phys. Soc.* **58**(2), 133 (1946).
7. J. C. GRENIER, thesis, Université de Bordeaux (1976).
8. J. C. GRENIER, F. MENIL, M. POUCHARD, AND P. HAGENMULLER, *Mater. Res. Bull.* **12,** 79 (1977).
9. J. C. GRENIER, G. SCHIFFMACHER, P. CARO, M. POUCHARD, AND P. HAGENMULLER, *J. Solid State Chem.* **20,** 365 (1977).
10. J. M. GONZÁLEZ-CALBET, M. VALLET-REGÍ, M. A. ALARIO-FRANCO, AND J. C. GRENIER, *Mater. Res. Bull.* **18,** 285 (1983).
11. A. A. COLVILLE, *Acta Crystallogr. Sect. B* **26,** 1469 (1970).
12. J. BERGGREN, *Acta Chem. Scand.* **25**(10), 3616 (1971).
13. J. C. GRENIER, M. POUCHARD, AND P. HAGENMULLER, *Struct. Bonding* **47,** 1 (1981).
14. Y. BANDO, Y. SEKIKAWA, H. YAMAMURA, AND Y. MATSUI, *Acta Crystallogr. Sect. A* **37,** 723 (1981).
15. J. C. GRENIER, L. FOURNES, M. POUCHARD, P. HAGENMULLER, AND S. KOMORNICKI, *Mater. Res. Bull.* **17,** 55 (1982).
16. M. MAREZIO AND P. D. DERNIER, *Mater. Res. Bull.* **6,** 23 (1971).
17. S. GELLER AND E. A. WOOD, *Acta Crystallogr.* **9,** 563 (1956).
18. M. A. GILLEO, *Acta Crystallogr.* **10,** 161 (1957).
19. E. F. BERTAUT AND F. FORRAT, *J. Phys. Radium* **17,** 129 (1956).
20. M. MAREZIO, J. P. REMEIKA, AND P. D. DERNIER, *Acta Crystallogr. Sect. B* **26,** 300 (1970).
21. B. G. HYDE AND L. A. BURSILL, *in* "Chemistry of Extended Defects in Non-Metallic Solids" (L. Eyring and M. O'Keeffe, Eds.), pp. 347–378 (especially pp. 375–378), North-Holland, Amsterdam (1970).
22. D. A. JEFFERSON AND J. M. THOMAS, *Mater. Res. Bull.* **10,** 761 (1975).
23. J. M. COWLEY AND S. IIJIMA, *Z. Naturforsch.* **27**(3), 445 (1972).
24. S. GELLER, R. W. GRANT, AND U. GONSER, *Progr. Solid State Chem.* **5,** 5 (1971).
25. U. SHIMONY AND J. M. KNUDSEN, *Phys. Rev.* **144**(1), 366 (1966).

26. C. R. A. CATLOW, J. M. THOMAS, S. C. PARKER, AND D. A. JEFFERSON, *Nature*, **295,** 658 (1982).
27. S. C. PARKER, *Solid State Ionics* **8,** 179 (1983).
28. Y. HIRUTSU, S. P. FAILE, AND H. SATO, *Mater. Res. Bull.* **13,** 895 (1978).
29. Y. HIRUTSU AND S. SATO, *Mater. Res. Bull.* **15,** 41 (1980).
30. Y. HIRUTSU, Y. TSUNASHIMA, S. NAKAGURA, H. KUWAMOTO, AND H. SATO, *J. Solid State Chem.* **43,** 33 (1982).
31. D. VAN DYCK, J. VAN LANDUYT, S. AMELINCKX, N. HUY-DUNG, AND C. DAGRON, *J. Solid State Chem.* **19,** 179 (1976).
32. T. J. A. DEN BRUEDER, *J. Solid State Chem.* **37,** 362 (1981).
33. S. ANDERSON, quoted by B. G. Hyde, in Ref. (*21*).
34. Y. TAKEDA, K. KAJIURA, S. NAKA, AND M. TAKANO, "Ferrites: Proceedings, International Conference, September 3, 1980, Japan" (H. Watanabe, S. Iida, and M. Sugimoto, Eds.), p. 414, Center for Academic Publications, Japan (1981).
35. M. TAKANO, N. NAKANISHI, Y. TAKEDA, AND T. SHINJO, "Ferrites: Proceedings, International Conference, September 3, 1980, Japan" (H. Watanabe, S. Iida, and M. Sugimoto, Eds.), p. 389, Center for Academic Publications, Japan (1981).
36. M. A. ALARIO-FRANCO, M. J. R. HENCHE, M. VALLET, J. M. G. CALBET, J. C. GRENIER, A. WATTIAUX, AND P. HAGENMULLER, *J. Solid State Chem.* **46,** 23 (1983).
37. M. A. ALARIO-FRANCO, J. M. GONZÁLEZ-CALBET, M. VALLET-REGÍ, AND J. C. GRENIER, *J. Solid State Chem.* **49,** 219 (1983).